CHARACTERIZATION OF A STAINLESS-CLAD STEEL REINFORCING BAR

Jonathon D. Tanks, EIT
Graduate Research Assistant
Virginia Center for Transportation Innovation & Research
Charlottesville, VA 22903
Telephone: (540) 847-9611
jdt5ca@virginia.edu

Stephen R. Sharp, PhD, PE
Senior Research Scientist
Virginia Center for Transportation Innovation & Research
Charlottesville, VA 22903
Telephone: (434) 293-1913
stephen.sharp@vdot.virginia.gov

Corresponding Author: Jonathon D. Tanks

Word Count: 3,109 words + 2 tables + 10 figures = 6,109 words

ABSTRACT

The concept of cladding traditional carbon steel reinforcing bars with stainless steel as a corrosion protection technique is theoretically economical: the mechanical properties and low cost of carbon steel is combined with the corrosion-resistant properties of stainless steel, with lower cost due to the small amount used compared to solid stainless bars. However, attempts to manufacture a high-quality clad bar have often been unsuccessful since, in many cases, the cladding-core interface cannot maintain a bond strong enough to transfer tensile forces between materials. Additionally, gaps, crevices, or very thin spots caused issues with the corrosion resistance. This paper looks at a different stainless clad bar with a greatly improved interface. The mechanical properties were analogous to carbon steel, with a distinct yield point and good ductility. Extensive microscopic and spectroscopic analysis revealed the nature and integrity of the cladding and the interface, which was characterized as having a "transition zone" wherein the stainless and carbon steels diffuse sufficiently to form a strong mechanical bond. The yield strength, ultimate strength, and elongation meet the AASHTO MP 13 specification for Grade 420 (60) reinforcing bars. The cladding thickness also showed less variability around the circumference when compared to a different clad bar from a former VDOT project.

INTRODUCTION

Conventionally reinforced concrete has provided a means of producing long lasting highway bridges with a relatively low initial cost. Unfortunately, when the reinforced concrete is subjected to deicing or seawater salt, corrosion of the reinforcement can occur (Figure 1) and damage the structure. When corrosion damage occurs, this leads to additional bridge maintenance or can even shorten the overall life of the structure. Studies have shown that the costs associated with damage can be high and that the operational life is often strongly influenced by the relatively low-cost concrete reinforcement in a bridge *(1-2)*. As a result of the damage corrosion can induce in a bridge, numerous studies have resulted in an effort to curtail corrosion in reinforced concrete structures and reduce maintenance costs *(3-8)*.

FIGURE 1 Spalling of the concrete as a result of traditional steel reinforcement undergoing corrosion after years of exposure to salt.

One of the proposed solutions to mitigate corrosion in bridges is stainless steel clad reinforcement, which has been shown to resist corrosion much more than carbon steel *(8-10)*. Although this idea is appealing, research has unfortunately shown that producing stainless steel clad reinforcement can be challenging as corrosion resistance and the concrete/steel bond strength can be diminished if the fabrication of the clad bar is not properly done *(7,11)*. Figure 2 shows the unevenness of the stainless cladding on clad bars previously studied by VDOT *(12)*, a void between the stainless cladding and carbon steel core, with the bar in Figure 2a being in the as-received condition, as well as debonding of the two as a result of tensile testing (Figure 2b).

However, a manufacturer of stainless steel clad reinforcement in the USA recently indicated that changes in production have improved the bond between the stainless steel cladding and the carbon steel core which increases their ability to produce a higher quality product. According to the manufacturer, the new stainless steel clad reinforcement can be produced in a high production in-line mill, with the resulting corrosion resistant reinforcing steel having an inclusion-free interface between the stainless cladding and the carbon steel core, through a proprietary electrochemical deposition technique. This paper evaluates whether this new clad

bar product exhibits improved mechanical properties over a previously studied product that was manufactured using a hot-forming process with cladding made of stainless steel shavings *(12)*.

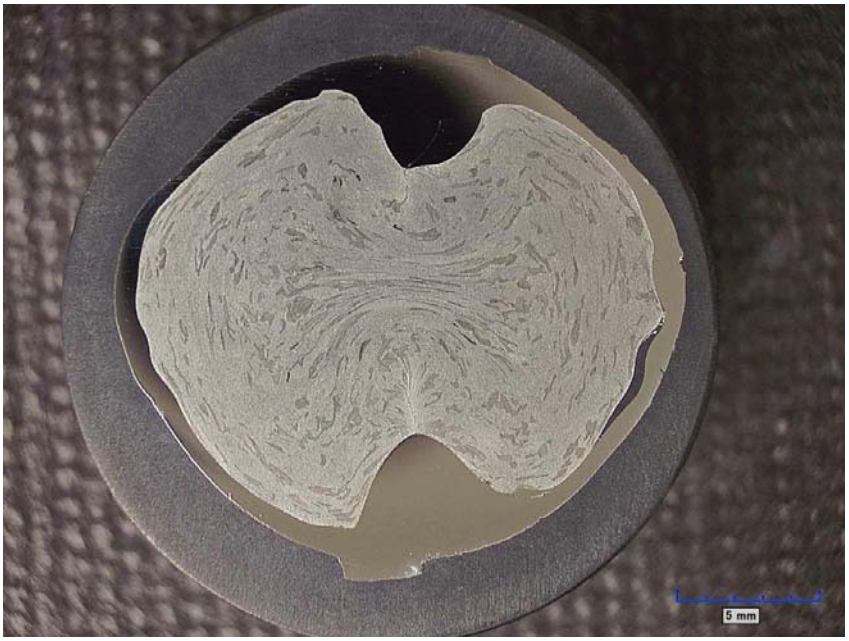

(a)

(b)

FIGURE 2 Sectioned view of a clad reinforcing bar showing (a) uneven cladding and debonding of stainless steel cladding layer from carbon steel core (dark slit along right side) and (b) separation of stainless steel cladding and carbon steel core during tensile testing.

EXPERIMENTAL APPROACH

The stainless clad reinforcing bar investigated in this paper (SC2) is a deformed 15.9 mm (0.63 in) diameter bar, and was compared to a different clad bar (SC1) of the same diameter. Currently, the manufacturer of SC2 can only provide bars of this size; other diameters are forthcoming. No machining or any other treatments were done to the material as part of this study. The characterization techniques used in this study include mechanical testing (uniaxial tension), scanning electron microscopy (SEM), optical microscopy (OM), and energy (x-ray) dispersive spectroscopy (EDS).

The tensile testing was completed with a servohydraulic universal testing machine with strain measured using a non-contact laser extensometer. A free-length of approximately 305 mm (12 in) and a gauge length of 5.1 mm (2 in) were used. Three specimens of SC1 and SC2 bars were tested, but complete stress-strain data was captured for one specimen each; only yield and failure values were recorded for the others.

Untested material was cut and polished, while the fracture surfaces of the tested specimens were preserved, for viewing with an SEM (FEI Quanta 650). For untested clad bar, samples were taken from bent sections (such as stirrups) and straight sections. To fully characterize the cladding thickness, as well as the transition layer at the cladding-core interface, EDS provided a reliable method for elemental analysis to quantitatively identify the material composition. Samples were polished but not coated for viewing in the SEM.

As a comparison to the SEM and EDS analysis of the cladding, a simplified measuring method was tested whereby the cladding was etched to enhance the cladding-core contrast. Samples were prepared following traditional metallography practices. Polishing was performed using 600, 800, and 1200 grit silicon-carbide paper. Etching was performed with a commonly used metallurgical etchant, 2% Nital. A digital optical microscope (Hirox KH7700) was used to capture the resulting micrographs with digital measurements taken at various locations.

RESULTS AND DISCUSSION

Tensile Properties

The average yield and ultimate strengths of SC2 were 445.8 MPa (64.7 ksi) and 696.6 MPa (101.1 ksi), respectively. Table 1 summarizes the average tensile properties of SC2 and SC1. The ultimate strain of SC2 was less than SC1, 14.6% compared to 26.1%, but is still greater than many common reinforcing steels and meets the 9% required minimum in AASHTO MP 13 (*13*). The results of tensile testing for representative SC1 and SC2 samples are presented in Figure 3, with an expanded linear-elastic portion to highlight the yield points.

Although a true elastic modulus does not exist for this material, which is a composite system, an apparent modulus is calculated from the stress-strain relationship in the linear elastic region of the graph. This is not an actual material property, but can be used for design purposes. For both SC1 and SC2 specimens, this value is considerably less than most carbon or stainless steels; it is possible that the cladding may deform at the surface slightly more than at the interface or the core, due to combined tension and shear that may occur from gripping the

specimen during testing. Considering that the elastic modulus of steel is about 210 GPa (29 msi) and the shear modulus is roughly 86 GPa (12.4 msi), an apparent modulus of 116-118 GPa (16.8-17.1 msi) would indicate that some multiaxial strain is recorded during the test. In future testing, a much longer free length (800-1000 mm) might give a modulus value closer to 210 GPa.

The distinct yield behavior of the SC2 is apparent in the graph, compared to the gradual elastic-to-plastic transition exhibited by the SC1, which is more similar to solid stainless steel. This was attributed to a very strong cladding-core interface in the SC2 while the SC1 experienced cladding-core debonding that led to ductile deformation of the stainless cladding and brittle fracture of the carbon steel core. The load carried by the debonded stainless cladding causes progressive plastic deformation, leading to the very high elongation displayed by SC1 in Figure 3. This can also be seen by the fracture surfaces in Figure 4, and the surface of SC1 is also shown in Figure 2.

TABLE 1 Average Tensile Properties of SC1 and SC2 Bar

Bar Type	Yield Strength	Tensile Strength	Apparent Modulus	Ultimate Strain
	MPa (ksi)	MPa (ksi)	GPa (ksi)	%
SC1	544 - 586 (79 - 85)	845.4 (122.7)	118.1 (17,130)	26.1
SC2	445.8 (64.7)	696.6 (101.1)	116.3 (16,880)	14.6

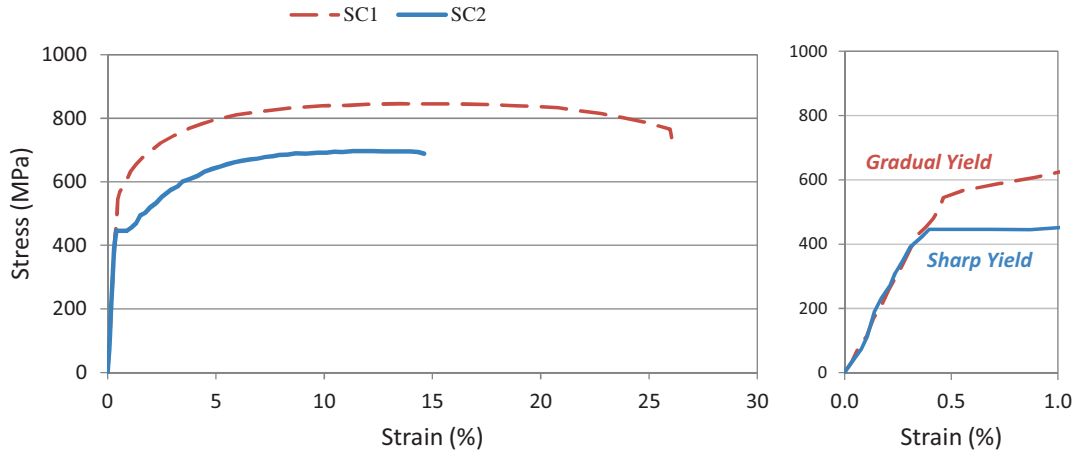

FIGURE 3 Mechanical behavior of old and new clad bar under uniaxial tension, with the yield point expanded on the right to show detail.

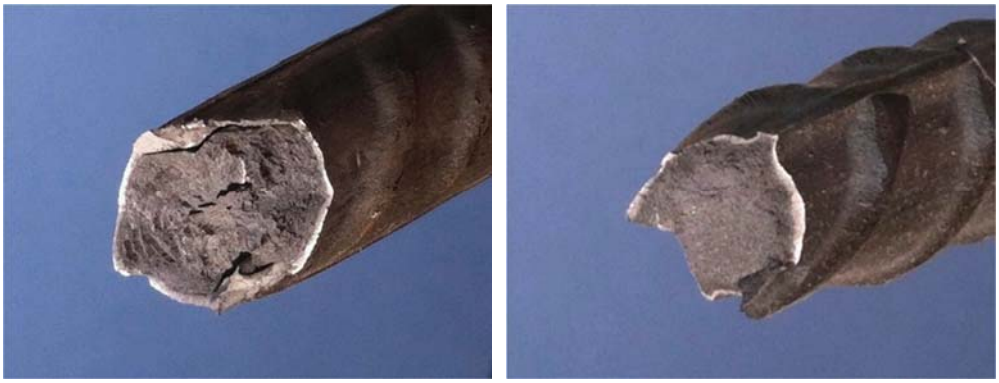

(a) (b)

FIGURE 4 Fracture surfaces after tensile testing, showing gaps between the cladding and core from debonding in SC1 (a) and the intact interface in SC2 (b).

Microscopic and Spectroscopic Analysis

To corroborate with mechanical testing, the SC2 bar was further characterized with SEM and EDS through microstructural and elemental analysis. Dimple patterns signifying ductile failure is present across the entire fracture surface, for both the core and cladding of SC2 bars. This is seen in Figure 5, with the core and cladding fracture faces of the SC2 specimen on the (a) and (b), respectively. On the other hand, only the stainless cladding failed in a purely ductile manner for the SC1 bars, with the core a mixture of ductile-brittle failure marked by mostly dimpling with some cleavage, shown in (c) and (d) of Figure 5, respectively.

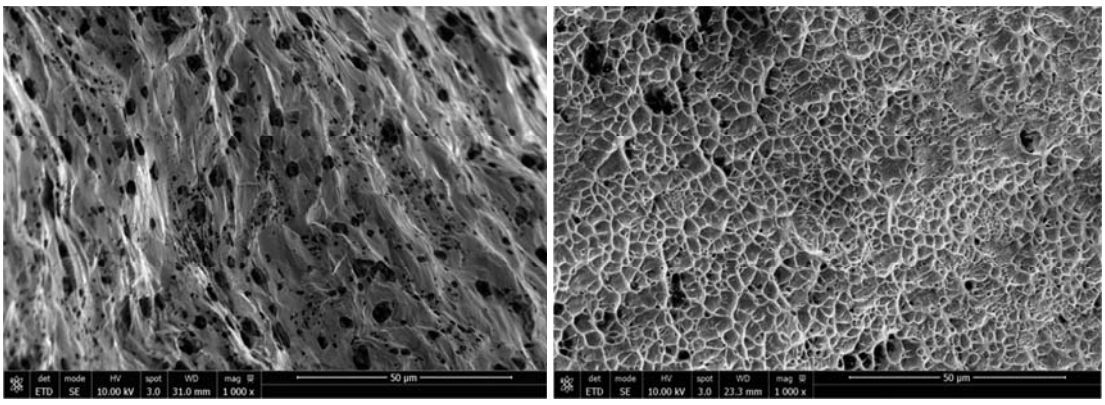

(a) (b)

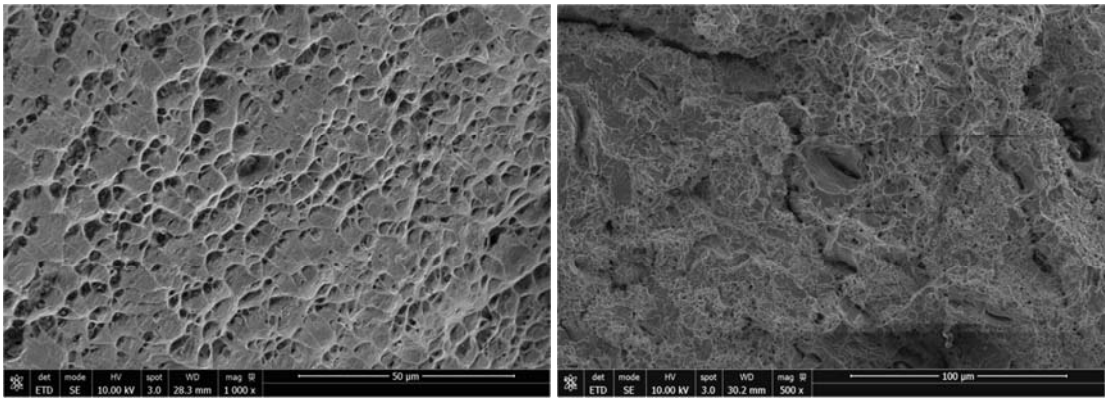

(c) (d)

FIGURE 5 Fracture surfaces for cladding (a) and core (b) of SC2, and cladding (c) and core (d) of SC1.

Since the cladding-core debonding is an issue with the SC1 bars, the integrity of the cladding-core interface all the way to failure with the SC2 bars is a significant feature. This comparison is made in Figure 6 between the SC1 (a) and SC2 (b) fracture surfaces. The gap seen in the SC1 bars averaged 150–300 μm, but no gaps were seen anywhere on SC2 specimens. A preliminary examination of bent SC2 specimens also showed an intact interface on the compression (inner radius) portion, seen in Figure 6c. The x-ray spectra from EDS analysis with respect to key elements in stainless steels, Cr, Ni, and Fe is illustrated in Figure 7.

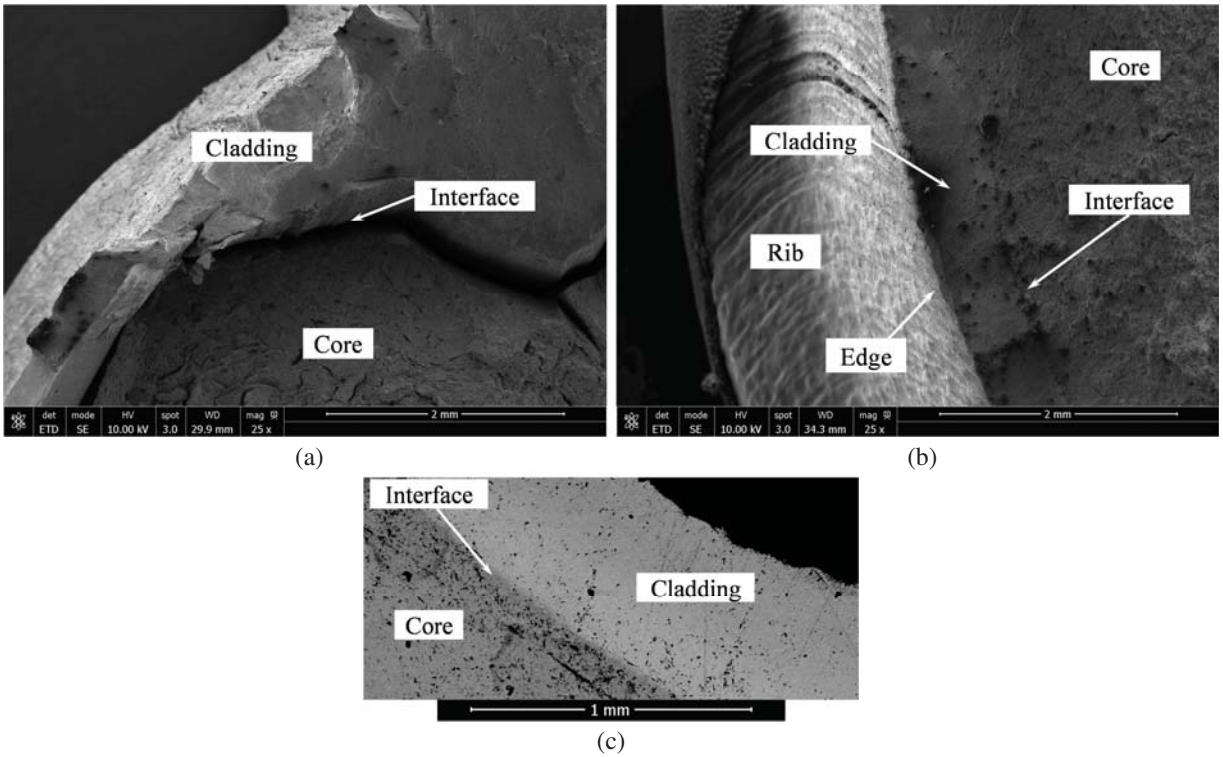

(a) (b)

(c)

FIGURE 6 Fracture surfaces of SC1 (a) and SC2 (b), showing interface condition, and interface at bend portion of SC2 in (c). Dark spots or streaks in (c) are from debris collected between SEM sessions.

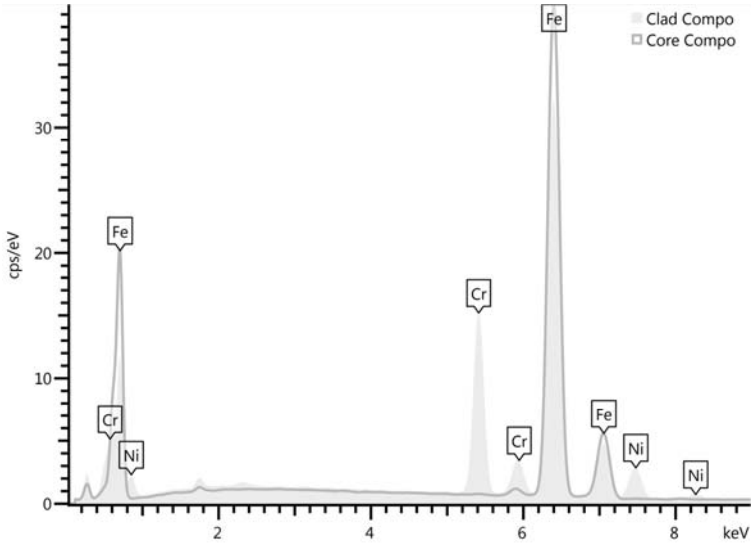

FIGURE 7 EDS spectra for cladding (shaded) and core (line) considering Fe, Cr, and Ni.

Evaluating Stainless Cladding Thickness

The cladding thickness and transition zone—referring to the diffusion of stainless and carbon steel at the interface to create a mixed layer—were also characterized with EDS. Key points of interest were the average, maximum, and minimum thickness, as well as consistency in thickness. Linescans allowed for elemental mapping of composition with respect to linear distances. Figure 8 contains linescans from a representative thick cladding area to determine the size of the transition layer. Poor quality cladding would leave a sharp interface with a very little diffusion, but the EDS analysis showed a consistently substantial transition layer, roughly 10 μm on average.

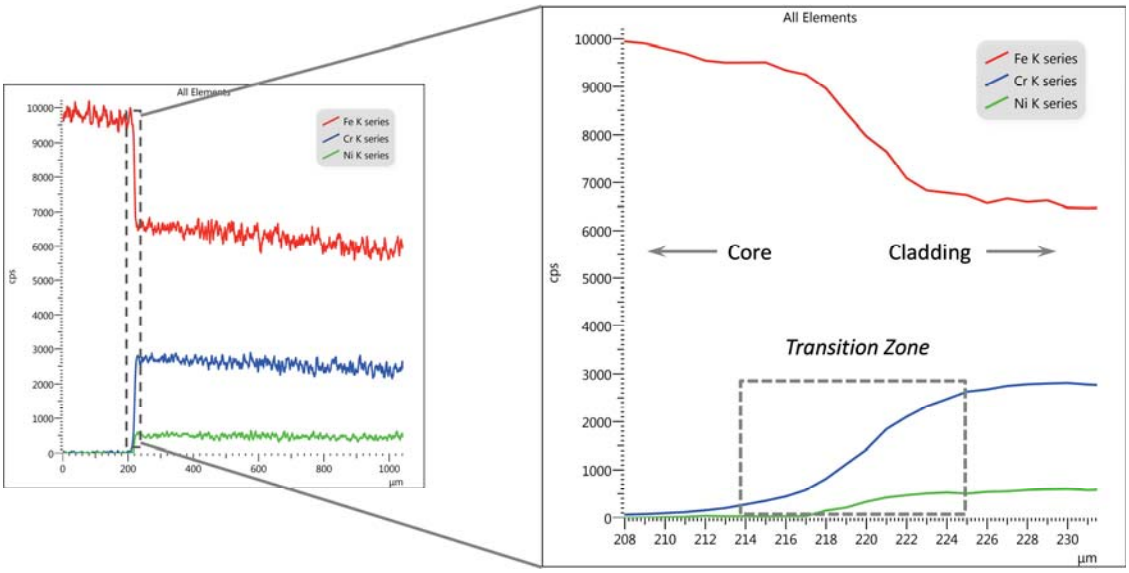

FIGURE 8 EDS linescan showing thickness of the transition layer between stainless steel cladding and carbon steel core, based on Fe, Cr, and Ni content in SC2.

SEM and digital OM were used in combination with digital dimensioning tools to visually measure the cladding thickness in several locations: thick areas (maximum) and thin areas (minimum), with and without lugs. A lug is the raised portion of the deformation pattern, whereas the shaft is the flatter recessed portion. EDS was also compared, using compositional rather than visual measurements. Cladding near lugs had much smaller thickness, as seen in Table 2. Examples of the SEM and OM measuring approaches are provided in Figure 9, where the Nital etchant clearly increases the contrast between the cladding and core. A statistical distribution is also included in Figure 10 for shaft and lug locations. A normal distribution with positive skew is evident, indicating a higher probability that variation in thicknesses will be seen mostly above the mean; i.e., values significantly greater than the mean are more likely than those less than the mean.

TABLE 2 Cladding Thickness Given by Various Measuring Approaches for SC2

	SEM		OM		EDS	
	Shaft	Lug	Shaft	Lug	Shaft	Lug
Min (μm)	787.1	234.4	904.9	292.8	906.4	310.0
Max (μm)	915.9	329.1	1276.8	527.1	1240.0	510.0
AVG (μm)	855.5	307.7	1067.0	400.8	1047.3	405.0
StDev (μm)	38.8	31.3	190.5	67.2	158.7	100.4
COV (%)	4.5	10.2	17.9	16.8	15.2	24.8

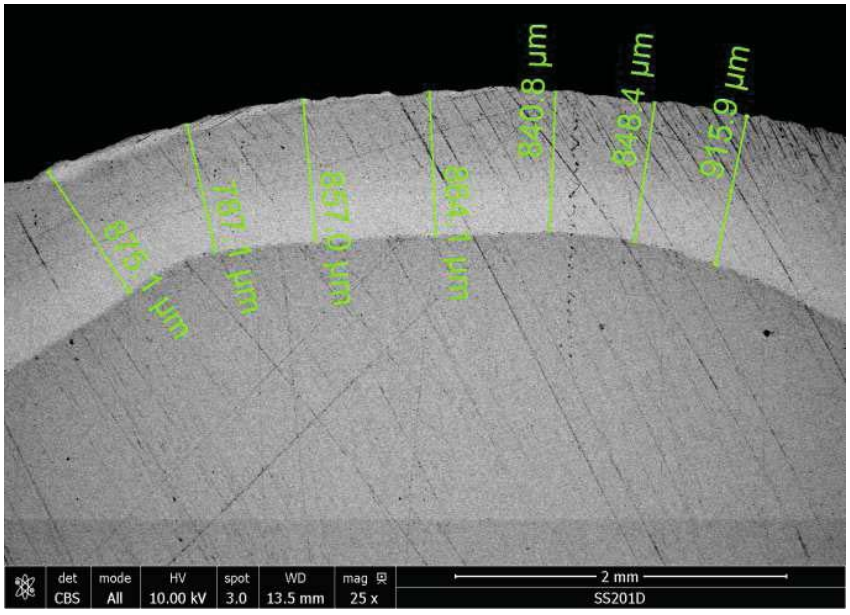

(a)

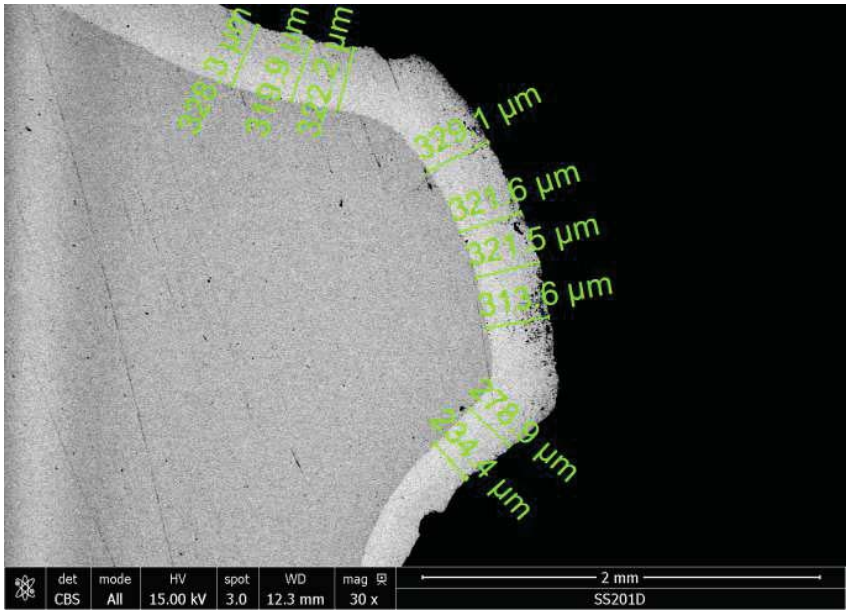

(b)

FIGURE 9 Measuring thickness of cladding in SC2 with backscattered SEM, with (a) shaft and (b) lug.

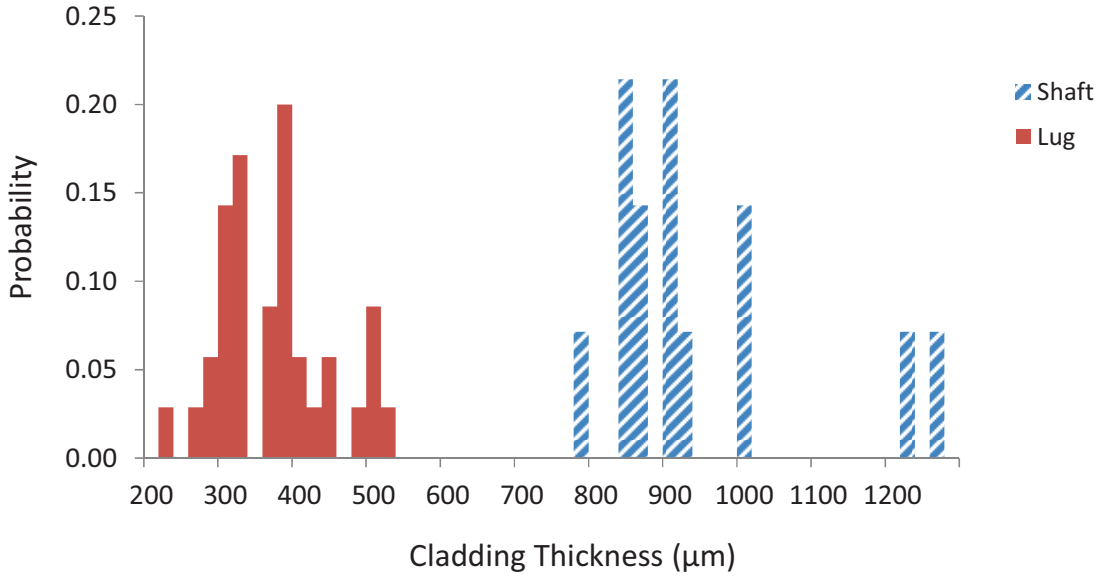

FIGURE 10 Statistical distribution of cladding thickness in SC2 for shaft (striped/blue) and lug (solid/red) areas.

Finally, the cladding thickness of the SC2 bar was more even around the reinforcing steel when compared to the previous SC1 bar. Figure 2 clearly indicates an uneven distribution of stainless steel around the carbon steel core for the SC1 bar. In this image, a very deep well of stainless steel is present in two locations, at the top and bottom of Figure 2a, and much thinner locations in other areas along the periphery. This unevenness is a concern regarding the corrosion resistance as well as cost of the stainless-clad reinforcement. Difficulties in

maintaining an even cladding layer are evident in the older generation bar and if the layer is too thin, as a result of trying to keep cost down, then corrosion could become an issue. The NC bar also exhibited variability in the thickness around the circumference, as previously discuss, but the distribution in the thickness was narrower for the SC2 bar. For both bars, however, AASHTO MP-13 states *(13)*,

"For acceptance purpose, at least 90% of all recorded thickness measurements of the cladding on the completed bar shall be a minimum of 175 μm [0.007"] on the completed bar."

Therefore, both bars exhibit sufficient cladding according to this standard.

CONCLUSIONS

A new stainless steel clad reinforcing bar was studied with respect to mechanical behavior under uniaxial tension, with material characterization of both the cladding and the interface. The following key points have been concluded from this investigation:

- Tensile properties for the SC2 bar meet the AASHTO MP 13 specification for Grade 420 (60) clad reinforcing bars, allowing for comparison to traditional reinforcing steels and other clad bar products.
- The SC2 bar exhibits a distinct yield point similar to traditional steel bars, with good ductility. This was attributed to a mechanically sound interface between the cladding and core, which maintained its integrity to the point of failure.
- The bond at the cladding-core interface was greatly improved in the SC2 bar compared to the SC1, ensuring the two materials maintain composite action under tension. EDS analysis verified the size and consistency of the transition zone at the interface. Furthermore, several methods were employed and compared for measuring the cladding thickness with good agreement.
- The SC2 bar exhibited less variability in the cladding thickness around the circumference when compared to the SC1 bar.
- The apparent elastic modulus was less than the expected value for steel, which might be attributed to shear strains on the surface of the cladding due to gripping during the test. Future work may include much longer free lengths to better determine the modulus.

Further work is needed before this material can be fully evaluated, primarily on its corrosion behavior in straight and bent conditions. Additionally, the issue with apparent elastic modulus should be addressed through more testing with various configurations; this is not a requirement for meeting the AASHTO MP13 specification, but is important for design purposes.

ACKNOWLEDGMENTS

The authors thank the Virginia Center for Transportation Innovation & Research for their support of this research, as well as Larry Lundy from the Materials Division of the Virginia Department of Transportation. Thanks also go to Richard White from the Department of Materials Science and Engineering at the University of Virginia.

REFERENCES

1. Koch, G.H., Brongers, P.H., Thompson, N.G., Virmani, Y.P, and Payer, J.H., *Corrosion Costs and Prevention Strategies in the United States*, Report No. FHWARD- 01-156, Federal Highway Administration, Washington, DC, March 2002.
2. Sharp, S. R., and A. K. Moruza. *Field Comparison of the Installation and Cost of Placement of Epoxy-Coated and MMFX 2 Steel Deck Reinforcement: Establishing a Baseline for Future Deck Monitoring*. Publication VTRC 09-R9. Virginia Transportation Research Council, Charlottesville, 2009.
3. Hartt, W.H., Powers, R.G., Leroux, V., and Lysogorski, D.K. A Critical Literature Review of High-Performance Corrosion Reinforcements in Concrete Bridge Applications Report No. FHWA-HRT-04-093, Federal Highway Administration, Washington, DC, July 2004
4. Darwin, D., Kahrs, J.T., Locke, Jr., C.E. Evaluation of Corrosion Resistance of Type 304 Stainless Steel Clad Reinforcing Bars, Report No. FHWA-KS-02-3, Kansas Department of Transportation, Topeka, Kansas, September 2002
5. Clemena, G.G., and Virmani, Y.P. Comparing the Chloride Resistances of Reinforcing Bars. Concrete International, Vol. 26, No. 11, pp. 39-49. 2004
6. Clemena, G.G., and Virmani, Y.P. *Testing of Selected Metallic Reinforcing Bars for Extending the Service Life of Future Concrete Bridges: Testing in Outdoor Concrete Blocks.* Publication VTRC 03-R6, Virginia Transportation Research Council, Charlottesville, 2002
7. Scully, J.R., Marks, C.A., and Hurley, M.F. *Testing of Selected Metallic Reinforcing Bars For Extending Service Life of Concrete Bridges In Solutions.* Publication VTRC 03-CR11, Virginia Transportation Research Council, Charlottesville, 2003
8. Cui F., and Sagüés, A.A. "Corrosion Performance of Stainless Steel Clad Rebar in Simulated Pore Water and Concrete", Paper No. 03310, 23 pp. Presented at Corrosion/2003, NACE International, Houston, 2003
9. Rasheeduzzafar, F., Bader, M., and Khan, M. Performance of Corrosion-Resisting Steels in Chloride-Bearing Concrete. ACI Materials Journal, Vol. 89, No. 5, pp. 439-448. 1992.
10. McDonald, D., Sherman, M., Pfeifer, D., and Virmani, Y. Stainless Steel Reinforcing as Corrosion Protection. Concrete International, Vol. 17, No. 5, pp. 65-70. 1995.
11. Sharp, S.R., Lundy, L.J., Nair, H., Moen , C.D., Johnson, J.B., and Sarver B.E. *Acceptance Procedures for New and Quality Control Procedures for Existing Types of Corrosion-Resistant Reinforcing Steel.* Publication FHWA/VCTIR 11-R21. Virginia Transportation Research Council, Charlottesville, 2011
12. Clemena, G.G., Kukreja, D.N., and Napier, C.S. *Trial Use of a Stainless Steel-Clad Steel Bar in a New Concrete Bridge Deck in Virginia*. Publication FHWA/VTRC 04-R5. Virginia Transportation Research Council, Charlottesville, 2003.
13. AASHTO MP 13, 2004, *Standard Specification for Stainless Clad Deformed and Plain Round Steel Bars for Concrete Reinforcement*. American Association of State Highway and Transportation Officials (AASHTO), Washington, DC, 2004.